ESI:

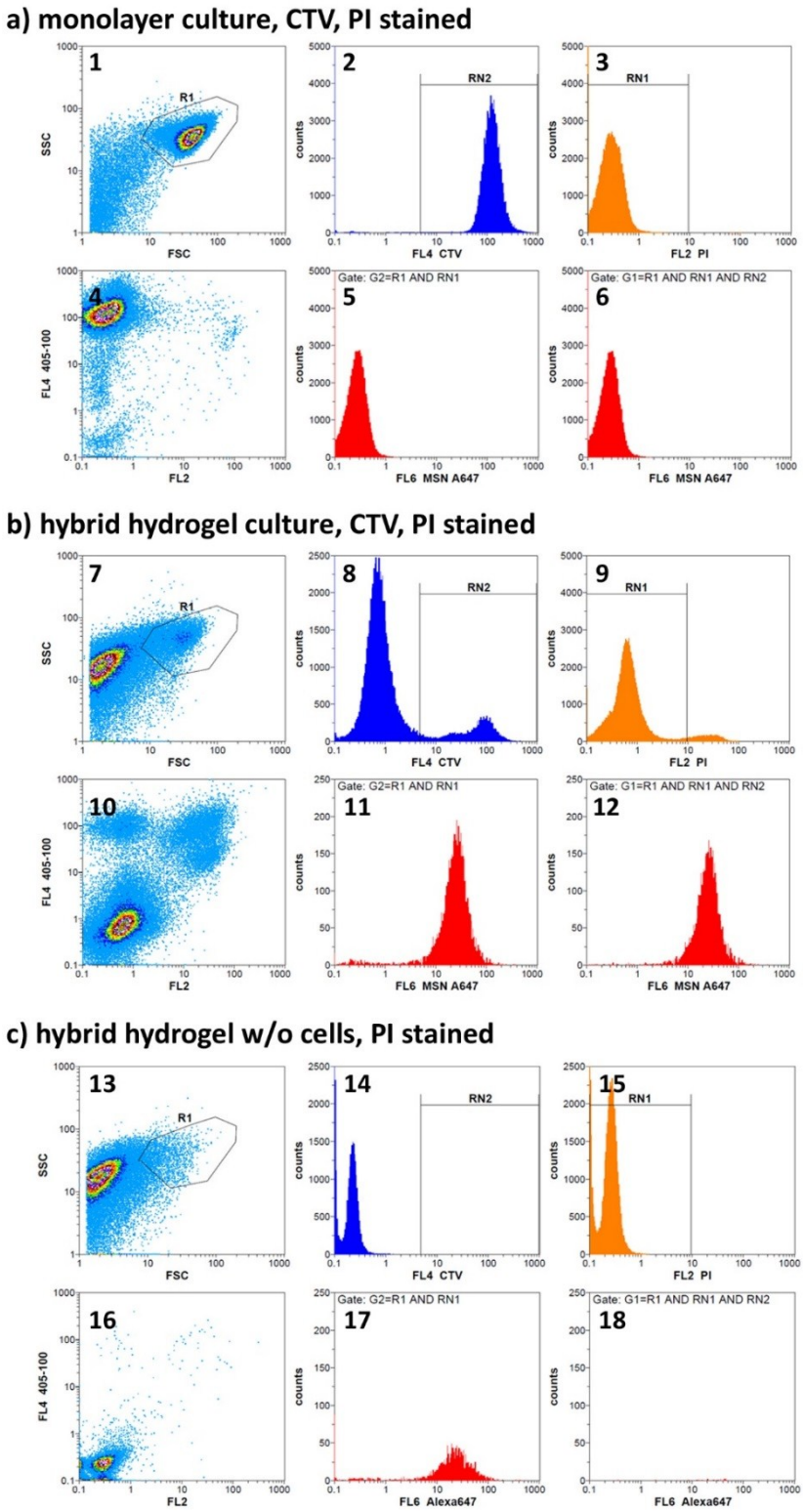

Fig. S1: Gating strategy for the flow cytometry based quantitation of particle uptake into MC3T3-E1 pre-osteoblasts from hybrid hydrogels. Live cells were identified basing on their forward (FSC) vs. side (SSC) scattering characteristics, which was set using a sample grown in conventional monolayer culture (region 1, R1), their negativity for the cell impermeable DNA intercalating dye propidium iodide (range 1, RN1 in FL2 histogram), and their positivity for the cell trace violet fluorescent dye (range 2, RN2 in

FL4 histogram), respectively. All events were analysed for simultaneous presence of these three criteria using a logical gate G1 including R1, RN1 and RN2. A second logical gate G2 included R1 and RN1, but excluded RN2 to demonstrate the necessity of CTV staining to distinguish between cells and hydrogel-derived particles. (a) Analysis of a CTV-stained control cell sample grown in conventional monolayer culture in the absence of Alexa647-labelled MSN. Plots 1, 2, and 3 show R1, RN1 and RN2, which were set basing on optical properties of the control sample. Histogram plots for red fluorescence (FL6) of events gated via G2 (plot 5) and G1 (plot 6) revealed background levels. (b) Logical gates were applied to flow cytometry analysis of a cell sample grown in hybrid hydrogel 3D culture in presence of Alexa647-labelled MSN. Plots 11 and 12 show red fluorescence (FL6) of events gated via G2 and G1, respectively. (c) Logical gates were applied to flow cytometry analysis of a sample prepared from a hybrid hydrogel which did not contain cells. Plots 11 and 12, as well as plots 17 and 18 show red fluorescence (FL6) of events gated via G2 and G1, respectively. Note that some events in plots 11 and 17 were false positively classified as cells when using logical gate G2 (FSC/SSC and PI negativity), but not when using logical gate G1 (FSC/SSC, PI negativity, CTV positivity, in plots 12 and 18). Thus, cell trace violet staining and analysis prevents the false positive classification of hydrogel-derived, Alexa647-positive particles.

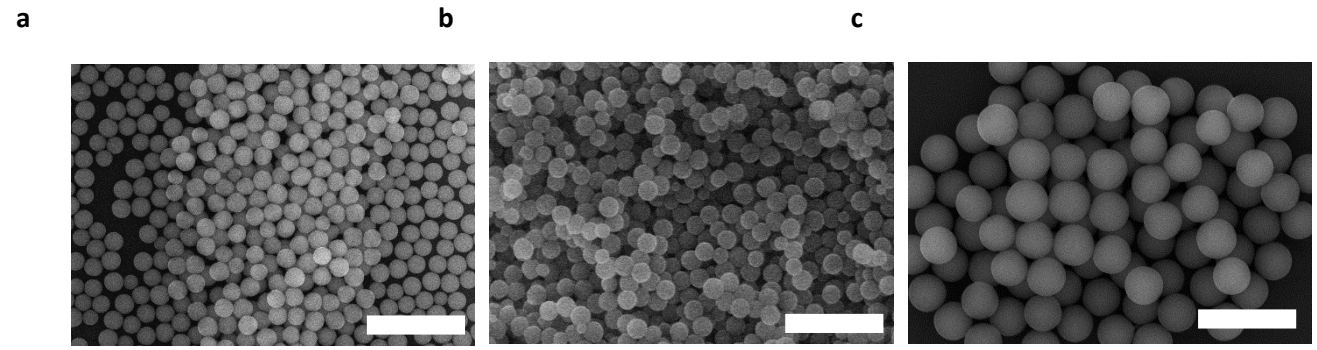

Fig. S2: SEM images of a) NP200-COOH, b) MSN200-COOH and c) MSN400-COOH. All scale bars refer to 1 µm.

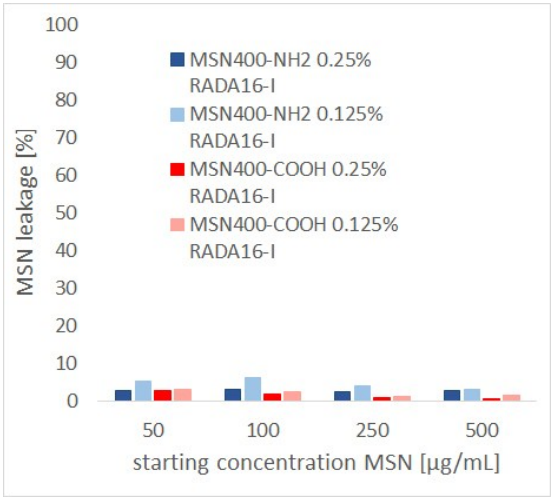

Fig. S3: MSN400 leakage from hydrogels with different RADA16-I densities was quantified via fluorescence spectrometry. Bars indicate percentages of MSN retrieval in the wash fractions generated during hybrid hydrogel equilibration.

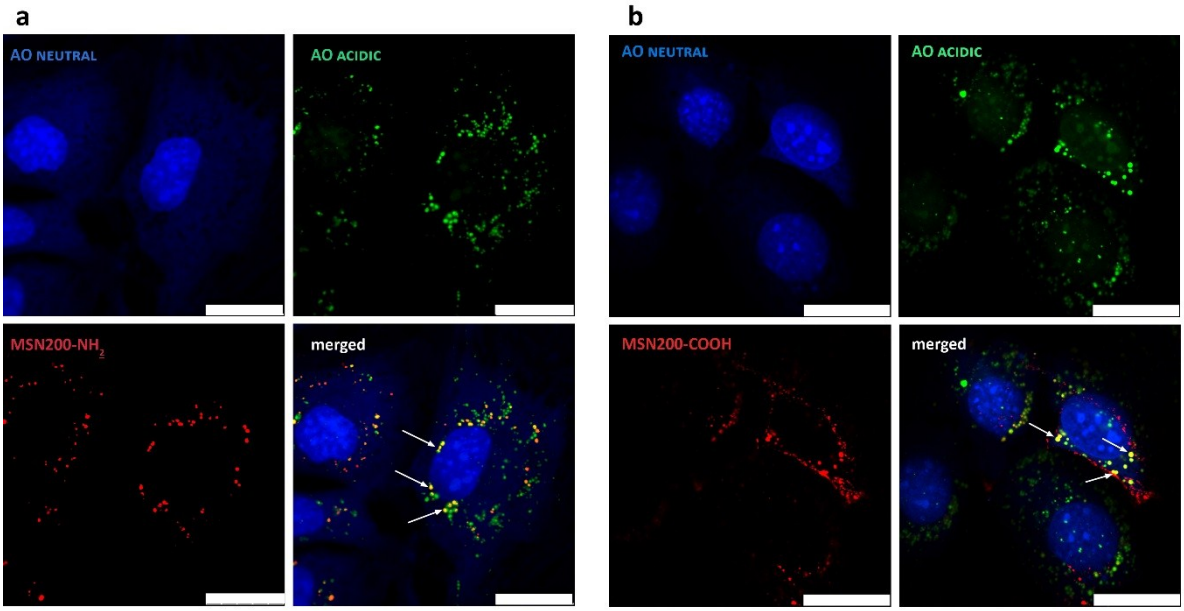

Fig. S4: Micrographs of MC3T3-E1 treated with (a) ATTO647N-labelled MSN200-NH_2 and (b) ATTO647N-labelled MSN200-COOH (100 µg/mL each) for 24 h. Live cells were counterstained using acridine orange (AO, 10 µM, 30 minutes at 37°C) and subjected to confocal Laser scanning fluorescence microscopy. Upon excitation with blue light (λ=488 nm), acridine orange emission depends on the pH of the cellular environment and thus can be utilized for labelling of acidic compartments such as endosomes, lysosomes, and vacuoles (Boya and Kroemer, Oncogene 2008, 27: 6434-51). Neutral compartments of the cell were detected by collecting emitted light at 493-547 nm (designated as "AO neutral"), whereas acidic compartments were detected by collecting emitted light at 575-739 nm (designated as "AO acidic"), respectively. Co-localization of MSN-derived fluorescence (in red) and AO acidic derived fluorescence (in green) results in yellow color and is exemplarily indicated by arrows. Scale bars refer to 25 µm.